RELATIONSHIP BETWEEN STRESS INTENSITY FACTOR AND ENERGY RELEASE RATE OF CHINESE-FIR

T Huang, F Wang, Z Shao* & Q Li

School of Forestry and Landscape, Anhui Agricultural University, Changjiang Road, No. 130, Hefei, China, 230036

**szp8@163.com*

Submitted August 2015; accepted November 2016

Compact tension specimen and double cantilever beam of Chinese-fir (*Cunninghamia lanceolata*) were used to measure stress intensity factor and energy release rate of opening cracks (mode-I) in tangential-longitudinal directions in crack body, respectively. The energy release rate was converted to stress intensity factor by Sih, Paris and Irwin relationship. The results showed no significant difference between the converted value of stress intensity factor and value measured by CT specimens. Thus, it is feasible to assume wood as an orthotropic elastic body and to apply the theory of fracture mechanics.

Keywords: *Cunninghamia lanceolate*, wood, mode-I crack, fracture mechanics, SPI relationship

INTRODUCTION

Wood is the only natural plant material that is used directly as structural material. Wood has been widely used as a natural structural material since ancient times. Currently, the yield of timber is about 80.88 million m^3 $year^{-1}$, equivalent to steel (China's National Bureau of Statistics 2014). Timber is used as structural material, such as beams, shed frame, floors and supporting body. However, defects and cracks exist naturally in wood. Thus, it is of great significance to analyse the fracture behavior and toughness by using fracture mechanics theory and methods, for design and safety (Shao 2012).

Research on wood fracture mainly focuses on tangential-longitudinal (TL) direction and radial-longitudinal (RL) direction cracks, since most cracks and defects formed during growth and processing are in the fibre direction. However, the resistance of wood against propagation of cracks along fiber direction is minimum. Wood shows strong anisotropic properties in stiffness and strength due to the external load or tension caused by ambient conditions, such as humidity and temperature. However, it is negative in the vertical direction of fiber. The TL crack propagation is similar to radial shake of wood, while the RL fracture propagation is similar to ring shake of wood. Therefore, in wood fracture mechanics, it is important to study the form and propagation of cracks caused by tension along the wood grain.

There are two methods to evaluate the fracture process of materials (Pineau & Joly 1991, Pineau 1992, Mamadou Méité et al. 2013). One is a local approach based on stress and strain concentrations in the crack tip neighborhood, while the other is a global approach, such as energy release rate, stress intensity factor and crack tip opening displacements (Budiansky & Rice 1973, Sih & Macdonald 1974, Kanninen et al. 1979). The macroscopic fracture criterion used in wood materials is divided into two categories, i.e. 1) criterion based on energy principle, such as energy release rate (G) and 2) criterion based on strength of the fracture tip strain zone, such as stress intensity factor (K) (Laren and Gustafsson 1990, Stanzl-Tschegg et al. 1994, Ewing & Williams 1979, Barrett & Foschi 1977). However, wood possesses many distinctive features compared with other orthotropic materials, due to its construction and structure. The high degree of uniformity and non-heterogeneous orientation in three principal directions pose a challenge to the application of fracture mechanics (Shao et al. 2002). Stanzl-Tschegg et al. (1995) studied the fracture energy of spruce wood in TL and RL directions with a new splitting method, and the size effects on K and G were investigated. Rostand et al. (2011) proposed a mixed-mode fracture specimen for wood, i.e. a combination of improved double cantilever beam (DCB) and compact tension (CT) specimen, to obtain fracture parameters for different mixed-mode configurations. Rathke et al. (2012) studied the energy release rate and stress intensity factor of wood based panels using fracture mechanics, but did not discuss the relationship between G and K. Pop et al. (2013, 2016) evaluated the fracture parameters of wood under mixed-mode loading by experimental and numerical methods. Shi et al. (1965) proposed the relationship between critical stress intensity factor and energy release rate called SPI relationship, showing its validity in orthotropy, plane strain conditions and linear elastic behavior. Triboulot et al. (1984) converted the experimental measured G to K by finite element method and analytical method according to SPI relationship to demonstrate its feasibility to treat wood as orthotropic and elastic body, and that fracture mechanics was applicable to wood. Although the converted values of K of two sample types were in accordance, no experiment was performed to verify the SPI relationship. Thus, it is not known whether the critical stress intensity foctor of delaminating fracture (K_{IC}) values obtained through different test methods are in agreement.

In this study, Chinese-fir was chosen to study the relationship between G and K. Due to the straight texture and uniform structure of Chinese-fir, after air drying, its stress–strain curve showed linear elastic properties, when loaded. Thus, to verify if Chinese-fir can be regarded as orthotropic material, CT specimen of Chinese-fir was used to measure the K of mode-I TL crack body. Then the DCB specimen was used to measure the G factor of mode-I TL crack body by compliance calibration method. Finally, the results of the two experiments and the relationship between G and K were compared and analysed.

MATERIALS AND METHOD

Material

Chinese-fir (*Cunninghamia lanceolata*) was chosen as sample. As shown in figure 1, the size of CT specimen was W = 50 mm, B = 20 mm, e = 12.5 mm, a = 25 mm, H = 60 mm where W = size of specimen with no crack, B = width of specimens, e = distance between loading holes and the right side of specimen, a = length of initial crack and H = height of specimen.

A total of 30 samples were tested. The size of DCB was W = 260 mm, B = 22 mm, e = 12.5 mm, H = 84 mm. A total of 7 samples were tested. The moisture content of specimens was about 12%. Temperature and relative humidity in the laboratory was 20 °C and 60% respectively.

Theory

There are two views on the study of crack propagation law by linear elastic fracture mechanics. One is the intensity of stress field in the crack tip, believing that the critical state of crack propagation is the moment when K reaches the critical value of material. Thereby the fracture principle is called K criterion. The other is the view of energy balance, believing that the driving force of crack propagation is the energy released by components during crack growth. Thus, the fracture principle is called G criterion. Although the starting point of these two criterions are different, there is a relationship between G and K under linear elastic conditions. Taking mode-I crack of isotropic material as an example, the relationship between G and K is as follows (Li & Zhou 1990):

$$G_I = \frac{1}{E^*} K_I^2 = S^* K_I^2 \qquad (1)$$

In plane stress situation:

$$E' = E$$

In plane strain situation:

$$E' = E/(1 - \mu)^2$$

$$S' = \frac{1}{E'}$$

where S^* = equivalent compliance, E^* = equivalent modulus, G = energy release rate, K = intensity factor, E = elastic coefficient, μ = Poisson's ratio and S' = flexibility.

As previously reported, the relationship between K and G shows that K represents not only the intensity of the elastic stress field near the crack tip, but its square also determines the energy released by crack propagation. Therefore, K criterion is equal to G criterion when solving linear fracture problems. Studies on the stress field of a single crack tip in an orthotropic body showed that the crack was parallel to the symmetry plane, as the elastic constants

$S_{16} = S_{26} = 0$. The relationship between G and K, called SPI relationship, contains four independent elastic constants (Sih et al. 1965, Wu 1967, 1968):

$$G = K_1{}^2 S^*$$
$$S^* = \frac{1}{E^*} = (\frac{S_{11}S_{12}}{2})^{\frac{1}{2}} [(\frac{S_{22}}{S_{11}})^{\frac{1}{2}} + \frac{2S_{12} + S_{66}}{2S_{11}}]^{\frac{1}{2}} \quad (2)$$

where G = energy release rate, K = intensity factor, S^* = equivalent compliance, E^* = equivalent modulus and S = elastic constant. Substituting S_{ij} by engineering elastic parameters, equivalent compliance of mode-I crack body is expressed as (Sih et al. 1965; Wu 1967, 1968):

$$S^* = \frac{1}{E^*} = (\frac{1}{2E_L E_T})^{1/2} \times [(\frac{E_L}{E_T})^{1/2} + (\frac{2\frac{-\mu_{TL}}{E_T} + \frac{1}{G_{LT}}}{\frac{2}{E_L}})^{1/2}]^{1/2} \quad (3)$$

where S^* = equivalent compliance, E^* = equivalent modulus, E_L = elasticity modulus along longitudinal direction, E_T = elasticity modulus along tangential direction, G_{LT} = shearing modulus of elasticity and μ_{TL} = Poisson's coefficient.

The small value containing Poisson's ratio is neglected, and thus the equivalent compliance is expressed as follows (Sih et al. 1965; Wu 1967, 1968):

$$S^* = \frac{1}{E^*} = (\frac{1}{2E_L E_T})^{1/2} \times [(\frac{E_L}{E_T})^{1/2} + [(\frac{E_L}{2G_{LT}})^{1/2}]^{1/2} \quad (4)$$

$$E^* = \frac{1}{S^*} = \frac{(2E_L E_T)^{1/2}}{[(\frac{E_L}{E_T})^{1/2} + (\frac{E_L}{2G_{LT}})^{1/2}]^{1/2}} \quad (5)$$

where S^* = equivalent compliance, E^* = equivalent modulus, E_L = elasticity modulus along longitudinal direction, E_T = elasticity modulus along tangential direction, G_{LT} = shearing modulus of elasticity and μ_{TL} = Poisson's coefficient.

Although wood is an anisotropic porous biomaterial, when cutting a small rectangle piece at a certain distance from the pith, making its symmetry plane perpendicular to growth rings, it is seen as an orthotropic body under macroscopic scale (Coleman 1991). Thus, many studies have researched the fracture toughness of wood, especially on wood fracture propagation along the grain. Ashby et al. (1985) considered that when a crack peeled or layered in open mode along the grain, the fracture process was similar to the peeling of bonded points. Since the composition and structure of the cell wall had almost no difference in various types of woods, the energy absorbed per unit area is approximately a constant when peeled, under a given moisture content, for all types of wood. In the fracture process, energy is provided by the elastic energy released by the surrounding wood and applied load. Therefore, in the principle of energy balance, called Ashby relationship, the energy release rate of mode-I peeling is (Lorna and Michael 2003):

$$G_{IC} = \frac{K_{IC}^2}{E_R} \quad (6)$$

where E_R = Young's modulus in radial direction, K_{IC} = critical stress intensity factor of delaminating fracture and G_{IC} = critical energy release rate of delaminating fracture.

The test of crack propogation

Since wood possesses strong heterogeneity and variability, the results from different experimental methods differed. The construction difference of wood was the main factor that affected the relationship between K_{IC} and G_{IC}. Moreover, both had a relationship with the occurrence of a bridge. Chinese-fir possessed the characters of straight grain, uniform structure, little and very thin wood ray, and so no bridge occurred in the crack propagation test.

The test of critical stress intensity factor (K_{IC})

The CT method was used to determine the K of pure mode-I of wood. The CT method is simple and easy to perform on small sized specimens, particularly suitable for wood with small diameter class. In this experiment, the CT specimen wood was made according to standard, ASTME 399 (2009). To make a pre-crack, a straight slot along the grain with a length of about 30 mm was sawed, using a band saw. The slot was then cut forward, 1–2 mm, using a sharp blade. To obtain a naturally sharp crack tip, a wedge was pushed into the slot to make the crack propagate forward about 2 – 5 mm. Finally, CT specimen was sawed according to the size given above. Such a specimen with natural sharp crack tip matched well with the cracked wood beam in a TL crack system (Figure 1).

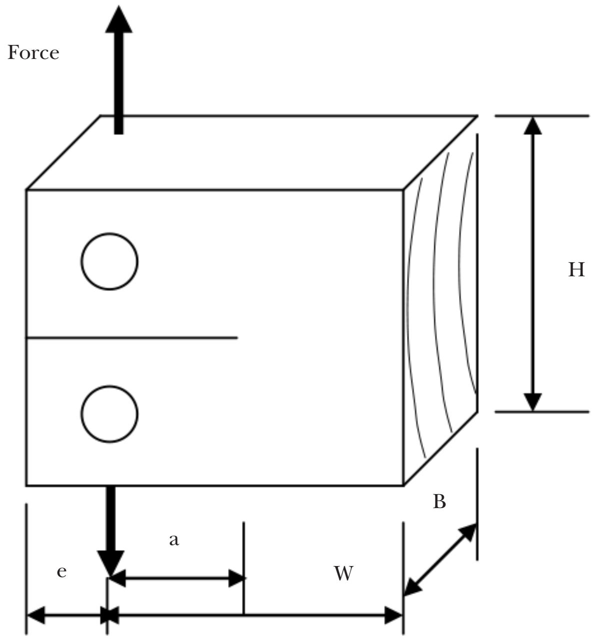

Figure 1 Compact tension specimen with tangential-longitudinal crack system

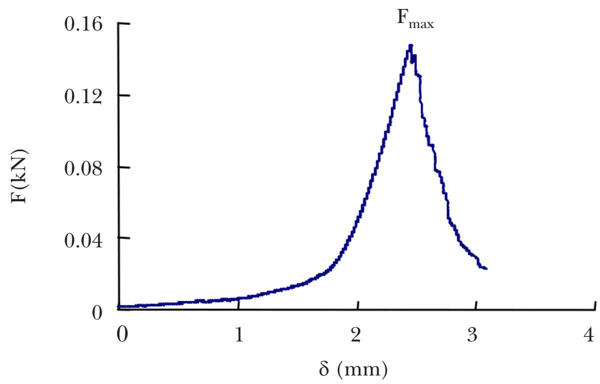

Figure 2 Load–displacement (F–δ) curve of compact tension specimen of Chinese-fir

The CT specimen was connected with a steel U hook using a steel pin loaded by the computer-controlled testing machine, with a crosshead speed of 2 mm min^{-1}. A computer recorded the load-displacement curve (F-δ) automatically, where δ = displacement between two load points. Air-dried wood presented brittleness. With an exception of the flat curve in the initial loading stage, caused by the space between the specimen and U-shaped hook, the F-δ curve was kept straight. Once the crack along the grain was initiated, unstable propagation happened, as seen in Figure 2. Therefore, the critical load (F_{max}) was substituted into the formula by ASTME 399 (2009), so that K along grain could be obtained (Sih 1973):

$$K_{IC} = \frac{F_{cr}}{B\sqrt{W}} \times f\left(\frac{a}{W}\right) \quad (7)$$

where F_{cr} = critical load, B and W = the size of specimens, as seen in Figure 1, aW^{-1} = dimensionless crack length and $f(aW^{-1})$ = specimen geometry function, given by the formula below (Sih 1973):

$$f(aW^{-1}) = 29.6(aW^{-1})^{1/2} - 185.5(aW^{-1})^{3/2} + 655.7(aW^{-1})^{5/2} - 1017.0(aW^{-1})^{7/2} + 638.9(aW^{-1})^{9/2} \quad (8)$$

The test of critical energy release rate (G_{IC})

The DCB specimen was used to determine the G_{IC} of pure mode-I critical strain of wood. The G_{IC} was calculated using compliance of crack, measured by the symmetrical bending test method. Triboulot et al. (1984) measured the fracture toughness of wood with TL-crack by DCB method, and compared it with finite element analysis (FEA), showing results that tallied with each other. In this experiment, the crack of DCB specimen was also a TL crack system (Figure 3), produced by the same method of CT specimen. The thickness of each specimen was more than 20 mm, and the fracture was regarded as a plane strain problem.

The tests were performed using a computer-controlled machine with a crosshead speed between 1 and 5 mm min^{-1}. At the beginning of the test, a low crosshead speed was used because the cantilever beams were short. Then the crosshead speed was increased when the cantilever beams were relatively long (Hodgkinson 2000). The computer recorded the curve of the applied load versus opening displacement (F-δ) automatically. The fracture of air-dried wood along the grain presented brittleness. With an exception of the curve in the initial loading stage, caused by the space between the specimen and U-shaped hook, almost all the F-δ curves remained straight. Once a crack along the grain was initiated, the crack propagation, parallel to grain, was unstable. The bearing capacity of the specimen decreased sharply, thus the top point of F-δ curve represented the critical point of rapid cracking. When the load decreased, the test machine was stopped and the recorded data was stored. The crack tips were marked

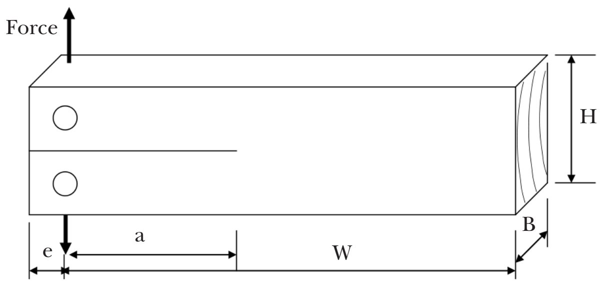

Figure 3 Sketch of double cantilever beam specimen

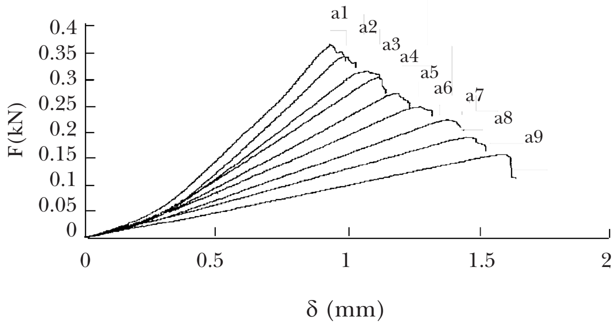

Figure 4 Typical load–displacement (F–δ) curve of double cantilever beam specimen of Chinese-fir

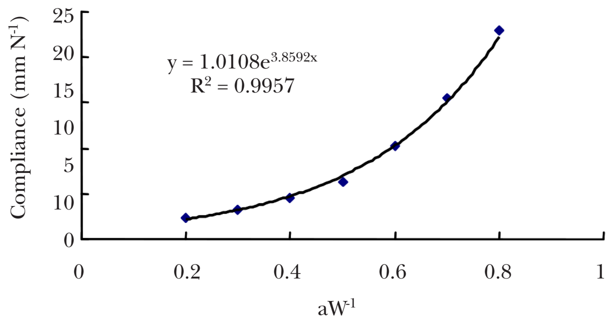

Figure 5 Relationship between compliance and dimensionless crack length (aW^{-1}) of double cantilever beam specimen of Chinese-fir

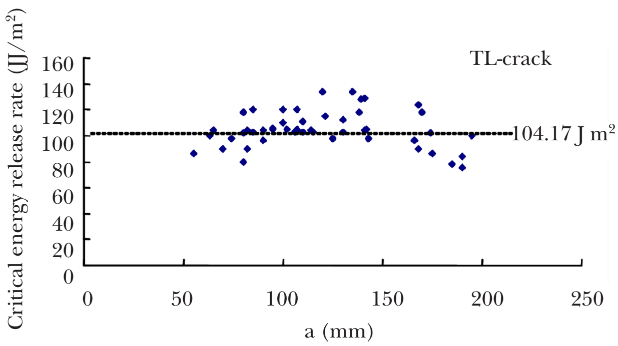

Figure 6 Relationship between critical energy release rate and a double cantilever beam specimen, TL = tangential–longitudinal, a = crack length

using an optical microscope. The specimens were then unloaded and reloaded. The same procedure was repeated until the specimen was fractured completely. The crack length, after each increment of delamination crack growth, was measured. The corresponding compliance (C_i) of the DCB specimen with a certain crack length (a_i) was calculated. Then exponential curve was chosen to characterise the relationship between compliance and crack length:

$$C = qe^{m(aW^{-1})} \quad (8)$$

where q and m = fitting coefficients of the compliance curve of the DCB specimen. By substituting the exponential equation of compliance into the following formula, the crack propagation resistance or G_{IC} of wood was obtained:

$$G_{IC} = \frac{F_{max}^2}{2BW} \times \frac{\partial C}{\partial(aW^{-1})} \quad (9)$$

where F_{max} = maximum force and C = compliance of F–δ curve.

RESULTS AND DISCUSSION

According to formula (7), CT specimens of Chinese-fir showed K_{IC} = 7.98 N mm$^{-3/2}$ (SD = 0.93 N mm$^{-3/2}$). Every DCB specimen was loaded and unloaded 6–9 times. The F–δ curves, corresponding to different crack length of a DCB specimen, and the relationship between the corresponding compliance and aW^{-1} are shown in Figure 4 and Figure 5. According to formula (8), G_{IC} of Chinese-fir TL crack system was 104.17 J m^{-2} (SD = 13.35 J m^{-2}), as shown in Table 1. The distribution relationship between G_{IC} and the responding crack length is shown in Figure 6. G_{IC} of Chinese-fir TL crack system had no obvious correspondence with the increase of crack length.

Measurements of elastic coefficient of Chinese-fir (Table 2) showed equivalent modulus, E^*= 661.50 N mm^{-2} in formula (3) and E_R = 520.00 N mm^{-2} in formula (6). The G_{IC} of DCB specimen was converted to K_{IC}, by SPI and Ashby relationship, $(K_{IC})_{DCB, SPI}$ = 8.29 N mm$^{-3/2}$

Table 1 The energy release rate of Chinese fir by double cantilever beam method

a (mm)	aW^{-1}	F_{max} (N)	C (mm N^{-1})	G_{IC} (J m^{-2})
49.5	0.19	366.28	1.69	87.37
59.5	0.23	341.27	2.05	89.27
71	0.27	313.61	2.6	90.93
82.5	0.32	302.07	3.01	101.75
95.5	0.37	273.31	3.64	102.96
107.5	0.41	247.8	4.52	102.93
120	0.46	221.68	5.61	100.99
137	0.53	188.14	7.23	95.97
155	0.6	156.75	9.73	89.33

a = crack length, aW^{-1} = dimensionless crack length, F_{max} = maximum load, C = compliance, G_{IC} = critical energy release rate

Table 2 The relationship between critical stress intensity factor and critical energy release rate (G_{IC})

Tree species	Crack system	K_{IC} (N $mm^{-3/2}$)	G_{IC} (J m^{-2})	SPI relationship		Ashby relationship	
		CT	DCB	$E^*=1S^{*-1}$ (N mm^{-2})	$K_{IC} = (G_{IC} E^*)^{1/2}$ (N $mm^{-3/2}$)	$E^* = E_R$ (N mm^{-2})	$K_{IC} = (G_{IC} E_R)^{1/2}$ (N $mm^{-3/2}$)
Chinese-fir	TL	7.98	104.17	661.50	8.29	520	7.35

$K_{IC =}$ critical stress intensity factor, $G_{IC =}$ critical energy release rate, S^* = equivalent compliance, E^* = equivalent modulus, E_R = Young's modulus in radial direction

(SD = 0.53 N $mm^{-3/2}$) and $(K_{IC})_{DCB, Ashby}$ = 7.35 N $mm^{-3/2}$ (SD = 0.47 N $mm^{-3/2}$).

The analysis of variance, as shown in Table 3, showed no significant difference between $(K_{IC})_{CT}$ and $(K_{IC})_{DCB, SPI}$. There was a fine equivalent relationship between K_{IC} and G_{IC} because no bridging occurred in the process of Chinese-fir crack, propagating along the grain. However $(K_{IC})_{CT}$ was significantly different from $(K_{IC})_{DCB, Ashby}$, the specimen being is TL crack system rather than TR type. The values of TR crack specimens had great variability due to unequal resistance, when crack propagated along earlywood and latewood, thus TL crack was chosen in this experiment.

Rectangular specimens was used to measure the elastic coefficients (E_L, E_T, G_{TL}, μ_{TL} and μ_{LT}) of wood by electrical measuring method, as shown in Figure 7. The shear elastic modulus (G_{ij}) was measured on specimen with 45° off-axis by applying the relationship between off-axis elastic constants and positive axis elastic constants as shown in formula (9).

$$Gij = E_X^{45^\circ}/2(1 + \mu_{xy})\ (I, j = L, R, T; i \neq j) \quad (9)$$

where G_{ij} = shear elastic modulus, $E_X^{45^\circ}$ = tensile elastic modulus of the specimen with 45° off-axis and μ_{XY} = Poisson's ratio.

However, there was a considerable distortion when the deformation of wood was delivered to the metal gate, because the modulus of resin matrix on strain gauge was higher than that of softwood. Therefore, the digital speckle method was applied to test the elastic coefficients. Artificial speckle was painted on the surface of the specimen, as shown in Figure 8 and Figure 9. The geometry position of corresponding points on two speckle images, collected before and after deformation of specimen, was recorded and calculated. The elastic coefficients were then calculated automatically by a computer. The elastic coefficients of Chinese-fir are shown in Table 4.

Table 3 Analysis of variance: single factor analysis of variance (SPI relationship and Ashby relationship)

Object	Differences source	SS	DF	MS	F	p-value	F crit
$(K_{IC})_{CT}$, $(K_{IC})_{DCB,\ SPI}$	Between groups	1.7510	1	1.7510	3.4560	0.0669	3.9668
	Within the group	38.5058	76	0.5067			
$(K_{IC})_{CT}$, $(K_{IC})_{DCB,\ Ashby}$	Between groups	7.4318	1	7.4318	15.8443	0.0002	3.9668
	Within the group	35.6479	76	0.4691			

SS = sum of squares of deviations, DF = degree of freedom, MS = mean square, F = the ratio of mean square, F crit = F test critical value

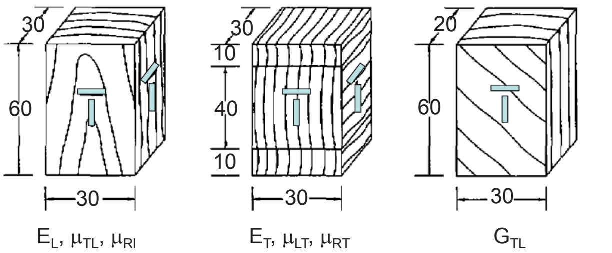

Figure 7 The specimens used to measure the elastic coefficient of wood by electrical measuring method

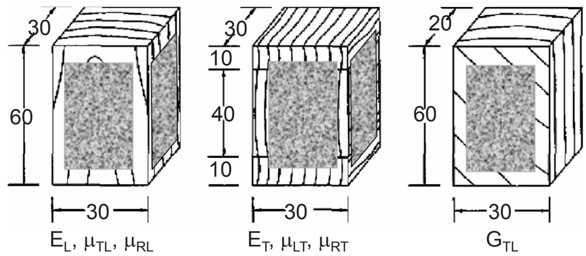

Figure 8 Group of three matched speckle specimens

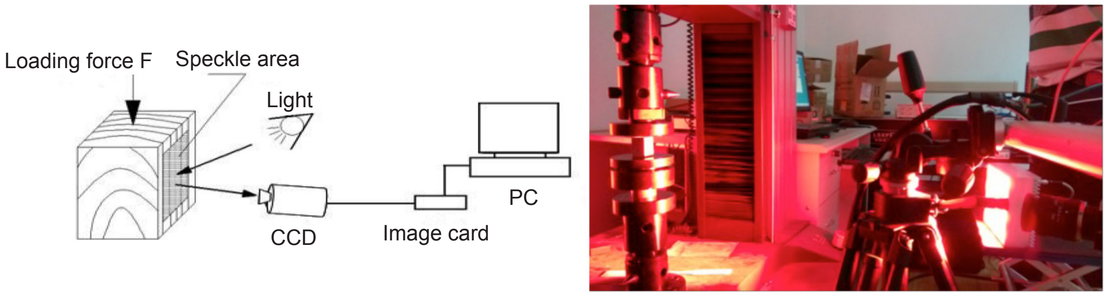

(a) (b)

Figure 9 Digital speckle method: a = schematic of test devices and b = experiment picture

Table 4 The elasticity modulus of Chinese-fir

Wood species	E_L (N mm^{-2})	E_R (N mm^{-2})	E_T (N mm^{-2})	G_{TL} (N mm^{-2})	S^* (mm^2 N^{-1})	E^* (N mm^{-2})
Chinese-fir	8500	520	300	106	0.00151	662

E_L = elasticity modulus along longitudinal direction, E_R = Young's modulus in radial direction, E_T = elasticity modulus along tangential direction, G_{TL} = shear modulus, S^* = equivalent compliance, E^* = equivalent modulus

CONCLUSIONS

In this study, CT and DCB specimens of Chinese-fir were used to measure K_{IC} and G_{IC} of mode-I TL crack body respectively. The results showed K_{IC} = 7.98 N mm$^{-3/2}$ (SD = 0.93 N mm$^{-3/2}$), G_{IC} = 104.17 J m^{-2} (SD = 13.35 J m^{-2}). Convertion of G_{IC} to K_{IC} by SPI relationship showed $(K_{IC})_{DCB,\ SPI}$ = 8.29 N mm$^{-3/2}$ (SD = 0.38 N mm$^{-3/2}$). There was no significant difference between the results of the two experiment methods. Thus it is feasible to assume wood as an orthotropic elastic body and to apply the concept of fracture mechanics.

ACKNOWLEDGEMENTS

The study was supported by the National Natural Science Foundation of China (No. 11008250).

REFERENCES

Ashby MF, Easter-Ling KE, Harrysson R & Maiti SK. 1985. The fracture and toughness of woods. *Proceedings of the Royal of Society London* 398: 261–280.

American Society of Tool and Manufacturing Engineers (ASTME) 399. 2009. *Standard Test Method for Linear-Elastic Plane-Strain Fracture Toughness K_{IC} of Metallic Materials*. ASTM International, West Conshohocken.

Budiansky E & Rice J. 1973. Conservation laws and energy release rates. *Journal of Appllied Mechanics* 40: 201–203.

Barrett JD & Foschi RO. 1977. Mode II stress-intensity factors for cracked wood beams. *Engineering Fracture Mechanics* 9: 371–378.

China's National Bureau of Statistics. 2014. *The People's Republic of China National Economic and Social Development Statistical Bulletin in 2013*. China's National Bureau of Statistics, Beijing.

Coleman. 1991. *Wood and Wood Process Principle*. China Forestry Publishing House, Beijing.

Ewing PD & Williams JG. 1979. Thickness and moisture content effect in the fracture toughness of Scots Pine. *Journal of Material Science* 14: 2959–2966.

Hodgkinson JM. 2000. Mechanical testing of advanced fibre composites. Woodhead Publishing Limited, Niklewicz.

Kanninen MF, Rybicki EF, Stonesifer RB & Broek D. 1979. Elastic-plastic fracture mechanics for two-dimensional stable crack growth and instability problems. *ASTM STP* 668: 121–150.

Li HS & Zhou CF. 1990. *Engineering Fracture Mechanics*. Dalian University of Technology Press, Beijing.

Laren HJ & Gustafsson PJ. 1990. The fracture energy of wood in tension perpendicular to the grain. Paper presented at the 23th CIB-W18 A Meeting, Lisbon.

Lorna JG & Michael FA. 2003. *Cellular Solids: Structure and Properties*. Tsinghua University Press, Beijing.

Méité M, Pop O, Dubois F & Joseph A. 2013. Characterization of mixed-mode fracture based on a complementary analysis by means of full-field optical and finite element approaches. *International Journal of Fracture* 180: 41–52.

Pineau A. 1992. Global and local approaches of fracture transferability of laboratory test results to components. Pp 197–234 in Argon AS (ed) *Topics Fract Fatigue*. Springer, New York.

Pineau A & Joly P. 1991. Local versus global approaches to elastic plastic fracture mechanics: application to ferritic steels and a cast duplex stainless steel. Pp 381–414 in Blauel JC & Schwalbe KH (eds) *Assessment in Components—Fundamentals and Applications, ESIS/EGF9*. Mechanical Engineering Publications, London.

Pop O, Dubois F, Méité M & Absi J. 2013. Characterization of wood fracture using optical full field methods. *Advanced Materials Research* 778: 440–447.

Pop O & Dubois F. 2016. Determination of timber material fracture parameters using mark tracking method. *Construction and Building Materials* 102: 977–984.

Rathke J, Sinn G, Weigl M & Müller U. 2012. Analysing orthotropy in the core layer of wood based panels by means of fracture mechanics. *European Journal of Wood and Wood Products*. doi: 10.1007/s00107-012-0635-6.

Rostand MP, Dubois F & Octavian P. 2011. A proposed mixed-mode fracture specimen for wood under creep loadings. *International Journal of Fracture* 167: 195–209.

Shao Z. 2012. *Fracture Mechanics of Plant Materials*. Science Press, Beijing.

Shao Z, Jiang Z & Ren H. 2002. The particularity of application of principles of linear-elastic fracture mechanics to wood and fracture parallel to grain. *Scientia Silvae Sinicae* 38: 110–115.

Sih GC & Macdonald B. 1974. Fracture mechanics applied to engineering problems-strain energy density fracture criterion. *Engineering Fracture Mechanics* 6: 361–386.

Sih GC. 1973. *Handbook of Stress Intensity Factors*. Leheigh University, Bethlehem.

Sih GC, Prais PC & Irwin GR. 1965. On cracks in rectilinearly anisotropic bodies. *Journal of Fracture Mechanics* 1: 189–203.

Stanzl-Tschegg SE, Tschegg EK & Teischinger. 1994. Fracture energy of spruce wood after different drying procedures. *Wood and Fiber Science* 26: 467–478.

Stanzl-Tschegg SE, Tan DM & Tschegg EK. 1995. New splitting method for wood fracture characterization. *Wood Science and Technology* 29: 31–50.

Triboulot P, Jodin P & Pluvinage G. 1984. Validity of fracture mechanics concept applied to wood by finite element calculation. *Wood Science and Technology* 18: 448–459.

Wu EM. 1967. Application of fracture mechanics to anisotropic plates. *Journal of Applied Mechanics* 34: 967–974.

Wu EM. 1968. Fracture Mechanics of Anisotropic Plate Composite Material Workshop. Pp 20–43 in Tsai SW, Halpin JC & Pagano NJ (eds) *Composite Materials Workshop*. Technomic Publishing Company, Lancanster.